Ann. Rev. Earth Planet. Sci. 1981. 9:81–111

MECHANICS OF MOTION ON MAJOR FAULTS[1]

Gerald M. Mavko
US Geological Survey, Menlo Park, California 94025

INTRODUCTION

Major faults are most simply viewed as the boundaries between lithospheric plates, across which relative plate motion is accommodated. On a global scale, these plate boundaries appear as simple zones of infinitesimal width; when averaged over thousands of years, the displacement rates are approximately steady. The simplicity disappears, however, when one looks in more detail. The surface fault trace is never a smooth break. The zone of concentrated strain may vary from a few meters to tens of kilometers wide. Furthermore, fault motion during the time scale of scientific observation is seldom simple. A section of a fault may exhibit a combination of nearly steady fault slip, episodic slip, minor seismicity, and large damaging earthquakes.

In spite of the complexity, a great deal of progress has been made toward understanding the mechanics of fault motion, primarily because of many careful field and laboratory observations and a few clever models. This paper reviews some of our current understanding of major earthquake cycles in terms of large scale fault models. The emphasis is on observable quasi-static deformation including the process of strain accumulation and the coseismic changes in static stress and strain. Several other reviews have recently been published on related topics, including mechanisms of earthquake instability and rupture (Dieterich 1974, Stuart 1978, 1979, Freund 1979), fracture mechanics applied to the crust (Rudnicki 1980), earthquake-related crustal deformation (Thatcher 1979), and rock properties (Kirby 1977, Tullis 1979, Logan 1979).

[1] The US Government has the right to retain a nonexclusive, royalty-free license in and to any copyright covering this paper.

ELASTIC REBOUND

Most theories concerning earthquakes are based on elastic rebound—the idea that elastic strain energy is gradually stored in the earth and is abruptly released during episodes of failure known as earthquakes. Comparisons of the accumulation of deformation at the earth's surface before large earthquakes with the rapid deformation during earthquakes show that they often approximately cancel except for a net rigid block translation of one side of the fault past the other. This led to the idea of a rebound (Reid 1910).

In the context of plate tectonics, the process of strain buildup and release at major plate boundaries repeats itself in a roughly cyclic fashion. The driving mechanism for the earthquake cycle is the relative plate motion across the common boundary (Andrews 1978). Whether or not strain accumulates, and the way it is released, depends on the nature of slip on the boundary.

We can describe a major cycle in terms of four time phases relative to the earthquake (Mescherikov 1968, Lensen 1970, Scholz 1972). In the *interseismic* or *strain accumulation* phase, the average fault slip on the plate boundary is slower than the long term average plate rate far from the fault. A simple geometric deficiency of slip accumulates causing strain energy to be stored in the plates on both sides of the fault. The *coseismic* phase is the period of several seconds to minutes during which rapid fault slip occurs, generating seismic waves. Most of the slip deficiency is recovered; stored elastic strain energy is converted into heat and waves (kinetic energy). The coseismic phase may or may not be preceded by a *preseismic* phase. This is a period of incipient strain release characterized by higher strain rates than occur during the strain accumulation phase. Rapid changes of any sort during this period might be interpreted as precursors. Finally the *postseismic* phase is a period of transient adjustment following the rapid earthquake movement. This adjustment may take place through aseismic creep, aftershocks, or viscoelastic relaxation.

Elastic rebound is also involved in the phenomenon known as fault creep. At several sites on the San Andreas and Calaveras faults in California, creep occurs in discrete aseismic events lasting up to several hours and separated by periods of little or no slip (Nason 1973). Creep events, like earthquakes, are episodes of strain release (C.-Y. King et al 1973, Goulty & Gilman 1978), although the amount and rate of slip are at least an order of magnitude less for a creep event than the amount and rate of slip for an earthquake with the same rupture length.

The short term unsteady slip associated with earthquakes and creep events is only a small perturbation superimposed on long term plate mo-

tion. In fact most strike-slip earthquakes are confined to only the uppermost 10–15% of a typical continental lithospheric thickness (although major thrusts include a larger fraction). Nevertheless, the unsteady slip excites transient deformation over a broad range of time scales, which forms the basis for most geophysical study of faulting.

COSEISMIC ELASTIC FIELDS

The best constrained portion of a rebound cycle is the rapid coseismic or strain release part. In general, we can determine from seismic and geodetic data the approximate area and orientation of the fault plane, the average slip, and the average stress change. This is possible primarily because the short term response of the earth to rapid fault slip is elastic. Therefore abrupt changes in strain due to earthquakes are insensitive to uncertainties in plate thickness and the inelastic rheologies responsible for long term plate motion. In this section we review some first order features of coseismic fault slip that are inferred from analysis of these elastic fields.

Dislocation and Crack Models of Faulting

Theoretical approaches to computing the static elastic fields due to faulting generally fall into two types: crack models and dislocation models. Crack models are based on a prescribed stress change on the fault plane (e.g. Starr 1928, Muskhelishvili 1953, Eshelby 1957, Knopoff 1958, Sneddon & Lowengrub 1969, Segall & Pollard 1980); dislocation models are based on a prescribed fault slip (Steketee 1958a,b). An advantage of the dislocation approach is the ability to compute the stress and displacement fields due to well-defined, arbitrarily shaped faults with arbitrary slip distributions. The deformation from complex slip distributions is constructed by linear superposition of simple slip solutions. The crack problem, on the other hand, involves mixed stress and slip boundary conditions in the plane of the fault and is generally more difficult to treat mathematically. Of course, both stress and slip changes accompany faulting, and the two descriptions are equivalent. Applications of this work to faulting have also been reviewed by Chinnery (1967) and Mavko (1978).

The most useful approach to modeling the displacement fields associated with three-dimensional faults is the dislocation formalism developed by Steketee (1958a,b). Steketee showed that if we approximate a fault as a discrete surface S of discontinuity (or dislocation) in an otherwise elastic half space, the resulting vector displacement U_k everywhere in the medium is given by an integral over the fault surface of point nuclei of strain τ_{ij}^k (Love 1944) multiplied by the local value of slip ΔU_i.

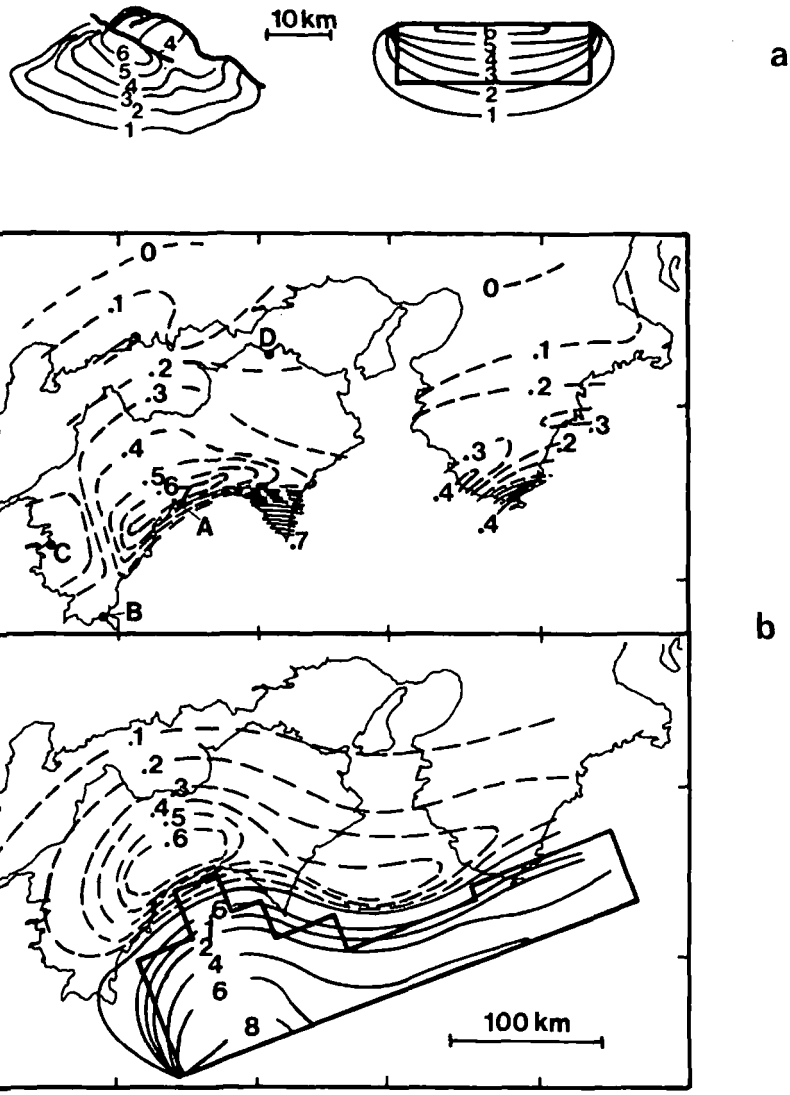

Figure 1 Contour maps comparing computed and observed surface displacement using rectangular fault models. (*a*) Observed (left) and computed (right) subsidence, in meters, associated with 1959 Hebgen Lake, Montana, earthquake (after Savage & Hastie 1966). Heavy rectangle shows the surface projection of the (normal) fault, which dips 54° S. (*b*) Observed (top) and computed (bottom) vertical displacement, in meters, associated with 1946 Nankaido, Japan, earthquake (after Fitch & Scholz 1971). Uplift is shown by solid contours; subsidence, dashed. Heavy polygon shows the surface projection of the (thrust) fault model, composed of six rectangular surfaces.

$$U_k = \frac{1}{8\pi\mu} \iint_S \Delta U_i \tau_{ij}^k \nu_j \, dS. \tag{1}$$

In Equation (1), μ is the elastic shear modulus and ν_j are the direction cosines of the normals to dS. The τ_{ij}^k are the displacements from a nucleus of strain in a half space and have been given in analytical form by Mindlin & Cheng (1950) and Maruyama (1964). Steketee's expression (1) is based on the concept of a dislocation surface composed of infinitesimal elements dS. Strains and stresses in the medium are obtained from the derivatives of (1) and Hooke's law.

A simple application of the formula (1) is the evaluation of displacements associated with uniform slip over a rectangular slip plane. The integral has been evaluated analytically and compared with observations for vertical strike-slip faults by Chinnery (1961, 1963, 1964, 1965) and for a variety of fault models, including dip-slip faults, by Maruyama (1964), Press (1965), and Savage & Hastie (1966). In fact, a rectangular fault with uniform slip is the most commonly used geodetic model of faulting. Examples of computed surface displacement for rectangular strike-slip and dip-slip faults are illustrated in Figures 1, 3, and 4.

A problem with uniform slip models is that they predict stress singularities around the edges of the fault. Furthermore, uniform slip is sometimes not sufficient to explain complicated surface deformation. Nonuniform slip on a three-dimensional fault requires numerical integration of Equation (1). Chinnery & Petrak (1967), for example, have evaluated the stress and displacements for a Gaussian distribution of slip over a roughly rectangular surface. However, in practice, strain fields from nonuniform slip are most often calculated by piecing together a finite number of rectangular fault patches, each with uniform slip (Fitch & Scholz 1971, Thatcher 1975, Dunbar 1977, Savage et al 1979).

Effects of variable slip and stress drop can be studied more easily in two dimensions. In two dimensions a very long fault (length $\gg$ depth) can be modeled as a distribution of elastic dislocation lines, screw dislocations when slip is parallel to the long fault dimension and edge dislocations when perpendicular (Weertman 1964, Bilby & Eshelby 1968, Mavko & Nur 1978). In contrast to Steketee's formalism, constructed from infinitesimal dislocation surfaces, each dislocation line marks the edge of a semi-infinite plane of slip. Variable slip $U(x)$, where x is the in-plane coordinate parallel to the fault (perpendicular to the dislocation line), is described by the dislocation density function $B(x) = -\partial U/\partial x$ where $B(x)\,dx$ represents the total length of Burgers vectors of the infinitesimal dislocations lying between x and $x + dx$.

The displacement field from a single dislocation in an infinite medium has a simple form (Weertman & Weertman 1964). For a screw dislocation lying along the z-axis with slip b parallel to the z direction, the only nonzero displacements are in the z direction:

$$U_z = \frac{b}{2\pi}\tan^{-1}(y/x). \tag{2}$$

For an edge dislocation lying along the z axis with slip b parallel to the x direction, the displacements are as follows:

$$\begin{aligned} U_x &= \frac{-b}{2\pi}\left[\tan^{-1}(y/x) + \frac{\lambda+\mu}{\lambda+2\mu}\frac{xy}{x^2+y^2}\right], \\ U_y &= \frac{-b}{2\pi}\left[\frac{-\mu}{2(\lambda+2\mu)}\log\left(\frac{x^2+y^2}{c}\right) + \frac{\lambda+\mu}{\lambda+2\mu}\frac{y^2}{x^2+y^2}\right], \\ U_z &= 0. \end{aligned} \tag{3}$$

Here λ is Lamé's coefficient and c is an arbitrary constant. The slip due to both types of dislocation is uniform over the half plane $y = 0$, $x > 0$. Because the material is linear and the elementary solutions (2) and (3) are invariant under spatial translation in an infinite medium the displacements due to variable slip are given by the convolution (Bracewell 1965) of (2) or (3) (with $b = 1$) with the distribution $B(x)$ (Canales 1975, Mavko & Nur 1978, Stuart & Mavko 1979).

The stress change in the plane of the fault is related to the slip through the Hilbert transform:

$$\sigma = \frac{\mu}{2\pi\alpha}\int_{-\infty}^{\infty}\frac{B(x')\mathrm{d}x'}{x-x'}. \tag{4}$$

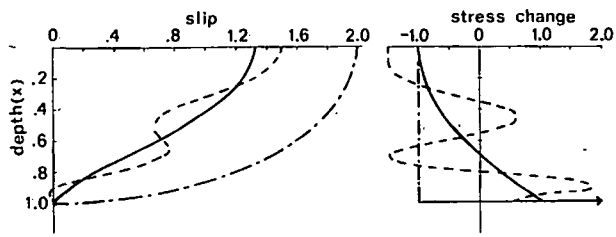

Figure 2 Three different stress-slip pairs for two-dimensional faults computed from Equation (4). Depth (x) can be interpreted as either distance from the center of a deeply buried fault, normalized by fault half width W, or actual depth, normalized by W, for vertical strike-slip faults breaking the surface. Stress is in arbitrary units τ. Displacement is in units of $\tau W\alpha/\mu$. Dashed and solid curves represent two heterogeneous fault models, both having the same moment. Dot-dashed curves represent the more familiar uniform stress drop model.

Here $\alpha = 1$ for screw dislocations, $\alpha = (1 - \nu)$ for edge dislocations, and σ is the component of shear stress in the direction of slip. The transform (4) can be evaluated numerically using the fast Fourier transform (Claerbout 1976, Mavko & Nur 1978, Stuart & Mavko 1979). Also, a large number of analytic transform pairs are given by Erdelyi et al (1954). Mavko & Nur (1978) outline a simple analytic procedure for inverting (4) for slip, given an arbitrary stress change σ expanded as a polynomial. Several stress-slip pairs for two-dimensional faults are shown in Figure 2.

A convenient feature of solutions constructed with screw dislocations is that a plane perpendicular to the fault (parallel to the dislocation lines) is traction-free whenever the slip is symmetric about the plane. Hence, the solution for a vertical strike-slip fault intersecting the free surface is just half of a full space solution constructed by mirroring the problem across the free surface (the method of images).

Geodetic Depth

A common feature of all static coseismic strain fields is that they rapidly decrease with distance from the fault, within several 10's of kilometers for strike-slip earthquakes and 100 km or so for major thrusts. Data showing the falloff of displacement with distance from the Nankai Trough (1946 Nankaido, Japan, thrust earthquake) and the Gomura Fault, Japan, (1927 Tango earthquake) are illustrated in Figures 1*b* and 3. The spatial scale of the strain release is a measure of the fault depth and can be understood in terms of the elastic models (Kasahara 1957, Chinnery & Petrak 1967).

Consider a very long (two-dimensional) vertical strike-slip fault in a half space with uniform slip D extending from the free surface to a depth W. The horizontal displacement $U(y)$ at the free surface is constructed from (2) using a buried screw dislocation and an image:

$$U(y) = \frac{D}{\pi}\tan^{-1}(y/W) \mp D/2. \tag{5}$$

(The sign $\mp$ is chosen: $-$ for $y > 0$ and $+$ for $y < 0$.)

The strain ε is the derivative $\delta U/\delta y$:

$$\varepsilon = \frac{D}{\pi W}\frac{1}{1 + (y/W)^2}. \tag{6}$$

The maximum surface strain and displacement occur at the fault trace, $y = 0$. The falloff of strain and displacement is scaled by the depth W, as illustrated in Figure 4*a*. Both U and ε drop to half their trace values at a distance $y = \pm W$, which gives a convenient surface measure of the depth

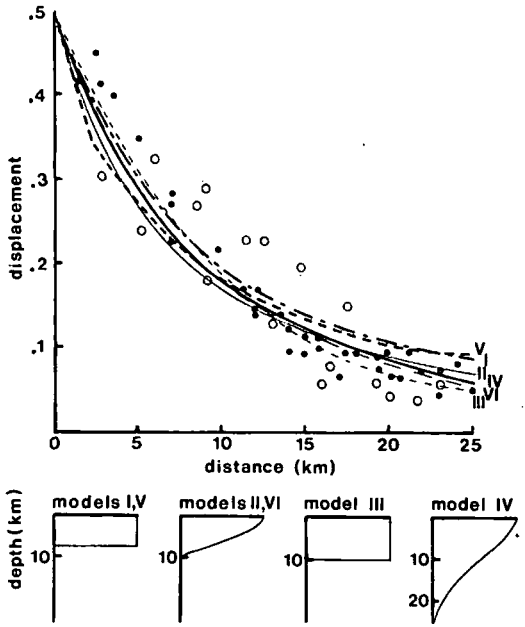

Figure 3 (*Top*) Computed and observed horizontal surface displacements associated with 1927 Tango earthquake. Closed circles—southwest side of the fault; open circles—northeast side (after Chinnery & Petrak 1967). Displacement is normalized by the trace offset; distance is perpendicular to the fault. (*Bottom*) Slip vs depth for six different fault models (see text).

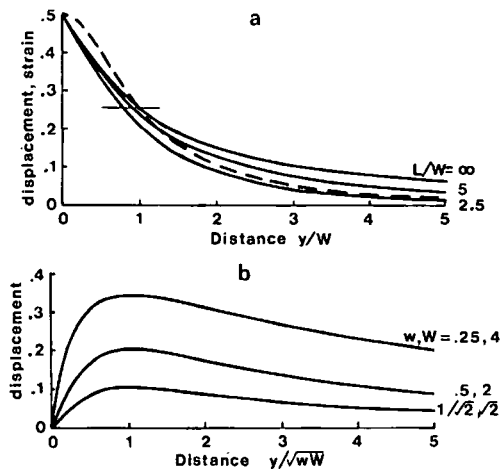

Figure 4 Falloff of surface displacement and strain with distance perpendicular to vertical strike-slip fault models. (*a*) Solid curves show displacement, normalized by the maximum trace offset, for rectangular faults with depth W and length L along the strike. Dashed curve shows shear strain for the two-dimensional case ($L/W = \infty$), arbitrarily normalized by twice the strain at the trace. (*b*) Surface displacement for three buried two-dimensional faults, all having the same mean depth, $\sqrt{wW} = 1$ and unit slip.

for this model. For faults with finite length L along strike, the displacement drops to half its trace value at a distance less than the depth.

Displacements computed for a variety of strike-slip models are compared with the observations from the 1927 Tango earthquake in Figure 3. In the figure, model I is the two-dimensional uniform slip model in Equation (5); model II is a two-dimensional model with slip smoothly tapering to zero with depth (Mahrer & Nur 1979); model III assumes uniform slip over a finite length rectangular fault (Chinnery & Petrak 1967); model IV assumes a rectangular fault with slip smoothly tapering toward zero near the edges (Chinnery & Petrak 1967). Clearly, a variety of uniform half-space models fits the data (the three-dimensional models fit a bit better than the two-dimensional ones) even though the scatter in the data is small. All of the models have a similar slip distribution of about 3 m in the uppermost 7 km, comparable to that predicted by the simplest two-dimensional model. Below 7 km, the models are quite different. This illustrates the general result that geodetic data can define the approximate depth range of greatest slip, but cannot constrain the details of slip (Weertman 1965, Chinnery & Petrak 1967). Details on a spatial scale d cannot be resolved at distances larger than d. Also the sensitivity of surface deformation to small amounts of slip decreases with depth (Thatcher 1978, Savage 1978), so that the estimated depth of faulting can be uncertain by a factor of two or more.

A more precise statement can be made about the models in Figure 3 by defining the geodetic depth as the depth of maximum slip gradient or the depth at which the slip falls to half the maximum value. In this sense the geodetic depths of the two-dimensional models I and II are within 2 km of each other and the depths of the three-dimensional models III and IV are within 4 km.

The simplest model for slip not breaking the surface is also two dimensional. The surface displacement and strain for a fault with uniform slip between depths w and W, not reaching the surface, is modeled with two dislocations and two images (Chinnery 1970):

$$U(y) = \frac{D}{\pi}[\tan^{-1}(y/W) - \tan^{-1}(y/w)], \tag{7}$$

$$\varepsilon = \frac{D}{\pi}\left[\frac{1}{W}\frac{1}{1+(y/W)^2} - \frac{1}{w}\frac{1}{1+(y/w)^2}\right]. \tag{8}$$

The displacement is shown in Figure 4*b* for several values of w and W. The position of maximum surface displacement, $y = \sqrt{wW}$ indicates the geometric mean of the upper and lower depths. The strain at the trace

Table 1 Geodetic depth and stress drop for strike-slip faults[a]

Earthquake	Magnitude	Depth (km)	Slip (m)	Reference	Stress drop (bars)
San Francisco (1906)	8.3	3.2	4.0	Knopoff (1958)	188
		6	5.0	Kasahara (1958)	125
		5	5.0	Chinnery (1961)	96
		12	4.9	Petrak (1965)	122
Tango (1927)	7.5	15	3.0	Kasahara (1958)	30
		15	3.4	Chinnery (1961)	37
		10	3.4	Chinnery (1961)	39
		25	3.4	Petrak (1965)	27
		20	3.4	Petrak (1965)	55
North Izu (1930)	7.0	8	4.0	Kasahara (1958)	75
		12	3.8	Chinnery (1961)	51
		26	3.8	Petrak (1965)	46
Imperial Valley (1940)	7.1	8	4.2	Kasahara (1958)	79
		6	4.2	Chinnery (1961)	69
		13	4.2	Petrak (1965)	96
		12	4.2	Petrak (1965)	106

[a] From a more complete table by Chinnery (1967).

and the far field displacement ($y \gg \sqrt{wW}, w - W$) are both proportional to the product $D(w - W)$. The depth range ($W - w$) can therefore be determined only if D is found independently. In practice, the fault area is often found independently from aftershock locations and slip is determined from the moment $\mu D(w - W)$.

Depths of faulting determined geodetically are shown for several strike-slip earthquakes in Table 1 (from a longer list by Chinnery 1967). The range of depths for each event results primarily from the range of models used to fit the data. An important result is that most strike-slip earthquakes are shallower than 10–20 km (Chinnery 1967, Eaton et al 1970a). The lack of deeper earthquakes has been attributed to a transition from stick-slip to stable sliding in the fault zone as the temperature increases with depth (Brace & Byerlee 1970) or to a general increase in ductility of the crust with depth (Lachenbruch & Sass 1973). Thrust faults show a larger scatter in rupture depths but are generally much deeper, particularly at subduction zones.

A complication in determining geodetic depth results from heterogeneity in crustal stiffness, which can distort surface strain fields. Rybicki & Kasahara (1977) and Mahrer (1978), for example, have found from theoretical studies that a relatively soft fault zone embedded in a stiff half

space will concentrate strain release closer to the fault than a uniform half space. This is illustrated as model V in Figure 3. Note the prominant knee in the curve illustrating the effect of the soft fault zone. Similarly Rybicki (1971) finds that a soft surface layer over a stiffer half space tends to concentrate strain closer to the fault for both surface and buried fault slip. Because fault zones and surface layers are usually less rigid than the surroundings, it appears that most geodetic determinations of fault depth, based on the falloff of surface displacements in a homogeneous half space, will be underestimated by as much as 50%.

As a counterexample, Mahrer & Nur (1979) have considered a half space with rigidity continuously increasing with depth (as opposed to a discrete soft layer over a half space) and find that the scale of surface displacements from strike-slip faulting is fairly accurately modeled by the homogeneous case (model VI, Figure 3). Chinnery & Jovanovich (1972) model faulting in a surface layer underlain by a shallow soft layer. This is one of the few plausible situations that would cause the geodetic depth, based on a uniform half-space model, to be an overestimate.

Seismic Moment and Stress Drop

An important static parameter of faulting that can be obtained directly from seismic observations is the seismic moment. In the far field at long periods a fault appears as a double couple point source. The scalar value of the moment of one of these couples is the seismic moment (Aki 1966). The seismic moment M_0 is a measure of the total final static slip ΔU on the fault surface S (Burridge & Knopoff 1964).

$$M_0 = \mu \iint_S \Delta U \, dS. \tag{9}$$

This is frequently rewritten in the form

$$M_0 = \mu \overline{\Delta U} S \tag{10}$$

where $\overline{\Delta U}$ is the average fault slip and S is the area of the slip patch. The average slip can be solved given an estimate of the rupture area S, for example, from the locations of aftershocks.

Brune (1968) showed that the contribution of seismic slip from many events to overall slip on a fault zone can be obtained from the sum of seismic moments. The average cumulative seismic slip from N events with individual moments M_{0i} distributed over fault area A_0 is

$$\overline{\Delta U}_0 = \frac{1}{\mu A_0} \sum_{i=1}^{N} M_{0i}. \tag{11}$$

Comparisons of seismic moments, Equation (10), with geodetic moments for individual earthquakes (N. King et al 1980) and cumulative slip, Equation (11), with long term geodetic slip rates (Brune 1968, Wyss & Brune 1968, Scholz et al 1969, Chinnery 1970, Langbein 1980) show that seismic slip is often much less than the total slip. Although there are uncertainties in computing moment and estimating rupture area, the differences are probably real and most likely indicate large amounts of aseismic slip.

In principle, the seismic stress drop can be computed from slip, using one of the dislocation theories, if the slip distribution is known in detail. However, the seismic moment and even geodetic data yield only the average slip from which only a certain weighted average of the stress change $\langle \Delta\sigma \rangle$ can be obtained. Seismologists usually assume the simple areal average of stress drop $\overline{\Delta\sigma}$ to be proportional to the average slip $\overline{\Delta U}$:

$$\overline{\Delta\sigma} = \frac{C\mu\overline{\Delta U}}{l}. \tag{12}$$

Here μ is the shear modulus, C is a numerical factor related to the shape of the fault, and l is a measure of the minimum fault dimension. Combining (10) and (12) yields a relation between stress drop and moment,

$$\overline{\Delta\sigma} = \frac{CM_0}{Sl}. \tag{13}$$

Values of C can be found from the ratio of average stress and slip predicted by the various crack and dislocation models. Using this method gives C of order unity for simple shapes and smooth distributions of stress and slip, although estimates will vary by a factor of 2 or 3 depending on the fault model used. For example, the value of C for the models in Figure 2 vary between .42 and .64 if $l = W$.

The uncertainty in inferring stress drop from moment is actually much worse when one considers realistic earthquakes having highly heterogeneous stress and slip distributions. Madariaga (1979) has shown that if the fault surface is planar and slip is everywhere parallel the scalar seismic moment in terms of variable stress drop is

$$M_0 = \iint_S \Delta\sigma E \, dS, \tag{14}$$

where the weighting function E is the slip calculated for a crack of the same shape but with a uniform stress drop $\Delta\sigma = \mu$. The expression (14) is valid for faults of any geometry, including multiple faults and heterogeneous stress drop. In the case of an elliptical fault, for example, with

semimajor and semiminor axes L and W

$$M_0 = \frac{3}{2} CW \iint \Delta\sigma \left(1 - \frac{x^2}{L^2} - \frac{y^2}{W^2}\right)^{1/2} dS,$$

$$= CWS\langle\Delta\sigma\rangle \tag{15}$$

where C is now a dimensionless constant that depends on the direction of slip and the ellipticity, $\varepsilon = W/L$, but not on the distribution of slip. The estimated stress drop $\langle\Delta\sigma\rangle$ is an average of the stress drop weighted with a function that emphasizes the stress near the center of the fault:

$$\langle\Delta\sigma\rangle = \frac{3}{2S} \iint \Delta\sigma(x, y) \left(1 - \frac{x^2}{L^2} - \frac{y^2}{W^2}\right)^{1/2} dS. \tag{16}$$

[Mavko & Nur (1979) independently derived the two-dimensional equivalent of (16) for the analogous problem of crack-opening under a heterogeneous pressure distribution.]

For heterogeneous stress drops $\langle\Delta\sigma\rangle$ will usually differ from the simple areal average $\overline{\Delta\sigma}$, though not by much (Madariaga 1979). Both $\langle\Delta\sigma\rangle$ and $\overline{\Delta\sigma}$, however, might be quite different from the actual stress drop. Madariaga considers the example of stress drop $\Delta\sigma_a$ at asperities covering a portion S_a of the total source area S. Assuming negligible stress drop in the rest of the plane the average stress drop is only a fraction of $\Delta\sigma_a$,

$$\langle\Delta\sigma\rangle \simeq \overline{\Delta\sigma} = \Delta\sigma_a S_a / S. \tag{17}$$

The localized or maximum stress drop at complex heterogeneous sources is usually underestimated by the average stress drop. Consider the stress drop on a two-dimensional fault expanded as a polynomial (Mavko & Nur 1978),

$$\Delta\sigma = \sum_{i=0}^{N} a_i T_i(x), \tag{18}$$

where T_i are Chebychev polynomials of the first kind (Abramowitz & Stegun 1964). The weighted stress drop $\langle\Delta\sigma\rangle$ obtained from the seismic moment is obtained from (18) substituted into (14). Because of the orthogonality of the polynomials only T_0 and T_2 contribute to the moment:

$$\langle\Delta\sigma\rangle = a_0 - a_2/2. \tag{19}$$

Wildly fluctuating stresses expressed in the form of T_i, $i \neq 0, 2$, contribute nothing to the moment, regardless of their amplitude. Simple examples are shown in Figure 2. The solid and dashed stress-drop curves correspond to the functions $\Delta\sigma = T_2$ and $\Delta\sigma = T_2 - T_8 + T_{12}/2$ respectively. Both have the same moment and the same average stress $\langle\Delta\sigma\rangle$ even though the

maximum stress drop is 50% greater and the maximum stress increase is 100% greater for the dashed function.

POSTSEISMIC, INTERSEISMIC, AND PRESEISMIC DEFORMATION

Observations of Transient Deformation

In a strictly elastic earth, complete elastic rebound would take place in a few seconds, with the characteristic time of strain release determined by the earthquake source rise time, fault dimensions, and rupture velocity. The only slow deformation would be the accumulation of tectonic strain. It appears, however, that an earthquake is often just a fraction of a larger episode of strain release. Pre- and postseismic transients are observed, which indicate a broad relaxation spectrum. For example, during the three years following the 1966 Parkfield, California, earthquake ($M = 5.5$; right-lateral strike-slip) as much as 25 cm of fault creep occurred at a decaying rate, although little or no surface breakage occurred during the main event (Smith & Wyss 1968, Scholz et al 1969). In addition, road damage occurring within several years before, and en-echelon cracks formed within a month before the earthquake (Allen & Smith 1966), suggest a preseismic transient. Rapid surface fault slip of more than 10 cm has occurred within several months following both the August 6, 1979, Coyote Lake, California, and October 15, 1979, Imperial Valley, California, earthquakes (J. Savage, personal communication, USGS 1980).

Even the great 1906 San Francisco earthquake, which led H. F. Reid to propose the elastic rebound mechanism, was followed by transient deformation. Thatcher (1975) suggests that substantial postseismic crustal strains, continuing for at least 30 years following the earthquake, can be inferred from geodetic surveys since 1906. These strains can be explained (though not uniquely) by $\sim$4 m of aseismic fault slip from 10 to 30 km depth, without additional surface slip. Thatcher (1975) also suggests anomalously rapid strain accumulation during the 50 years prior to 1906, although the evidence is weak (Savage 1978, Thatcher 1978).

Perhaps the most spectacular example of postseismic deformation was observed following the 1946 Nankaido, Japan, earthquake ($M = 8.2$; thrust type) where upheavals of as much as 2 m occurred over a 1 to 3 year period. Figure 5*a* (Matuzawa 1964, Kanamori 1973) shows the rather complicated nature, in space and time, of the vertical displacement. Similar deformations occurred during the 10 years following the 1964 Alaskan ($M = 8.4$; thrust type) earthquake (Brown et al 1977, Prescott & Lisowski 1977, 1980).

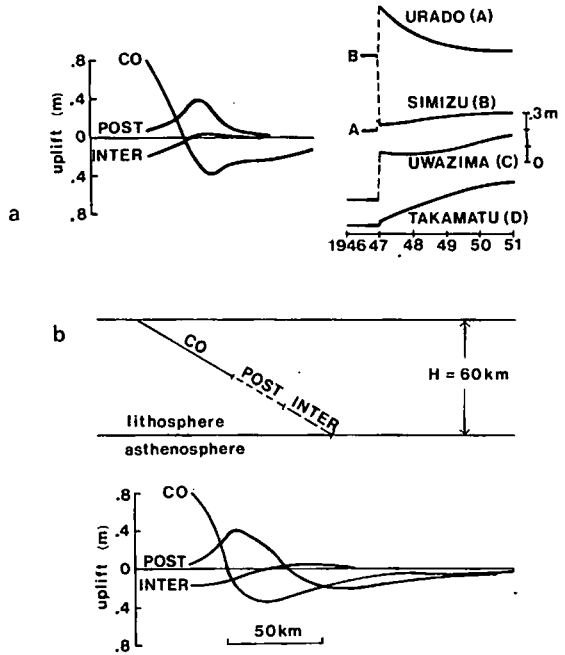

Figure 5 Observed and computed coseismic, postseismic, and interseismic vertical deformation associated with the 1946 Nankaido, Japan, thrust earthquake (after Fitch & Scholz 1971, Thatcher & Rundle 1979). (*a*) Observed profiles perpendicular to the Nankai Trough (*left*) and smoothed tide gage records (*right*) at locations labeled *A–D* in Figure 1*b*. (*b*) Two-dimensional model (see text) and computed profiles, both drawn to the same scale as the profiles, in (*a*).

Particularly short-lived transients have also been observed. Rapid fault slip lasting only several hours was recorded after a Matsushiro shock on September 6, 1966 (Nakamura & Tsuneishi 1967, Scholz 1972). A precursory aseismic slip with time constant of 300 to 600 s, starting about 1000 s before the main shock of the 1960 Chilean earthquake, has been inferred from long-period surface waves and body waves (Kanamori & Cipar 1974) and from free oscillations (Kanamori & Anderson 1975). Ando (1975), Sacks et al (1977), and Pfluke (1978) give evidence of earthquakes with geodetic moments several times that determined from seismic methods. Because large tsunamis were generated, the duration of the aseismic component of slip is apparently minutes to hours, long compared to the response band of seismographs but short compared to the response of the sea. Further examples of transient deformation are reviewed by Scholz (1972), Kanamori (1973), Dunbar (1977), Pfluke (1978), and Thatcher (1979).

Relaxation Mechanisms

An earthquake rupture superimposes a stress perturbation onto the preseismic state—decreasing the stress over much of the rupture area and increasing it elsewhere. As discussed earlier, these coseismic fields are now well understood, and numerous studies have shown that the associated abrupt displacements can be explained in terms of fault slip in an elastic medium. Postseismic observations suggest a subsequent viscoelastic response. A material is viscoelastic when its initial response to abrupt changes of stress or strain is elastic, while its longer term response is a viscous relaxation or flow (Fung 1965, Christensen 1971). Most rocks flow to relax shear stresses, as though the rigidity gradually decreases with time. Bulk relaxation is much less common.

What are the viscous elements? A simple mechanical model for the earth's crust and upper mantle, suggested by plate tectonics, consists of a relatively elastic, brittle lithosphere overlying a ductile asthenosphere. Within this framework we can distinguish geometrically three general sources of relaxation.

RELAXATION IN THE ASTHENOSPHERE The asthenosphere is characterized by high temperature relaxation mechanisms (Ashby & Verrall 1977, Weertman 1978, Tullis 1979). Solid mineral grains can flow plastically by atomic diffusion and the motion of lattice dislocations (Gordon 1965, Weertman & Weertman 1975, Heard 1976, Carter 1976). This makes the polycrystalline composite fluidlike over long time scales and can account for the large-scale, finite deformation implied by plate motion and the low strength implied by isostatic equilibrium. In addition, enhanced deformation at grain boundaries can occur resulting from dislocation motion and diffusion (Ke 1947, Zener 1948, Anderson 1967) or the viscous flow of melt (Walsh 1969, Mavko & Nur 1975, O'Connell & Budiansky 1977). Other loss mechanisms which are relevant at seismic frequencies include thermoelasticity, dislocation damping, point defect diffusion, and grain boundary effects (Anderson 1967, Jackson & Anderson 1970).

RELAXATION IN THE LITHOSPHERE The lithosphere, by definition, is a relatively strong, rigid layer that can resist permanent deformation or plastic flow for long periods of time, whereas the asthenosphere cannot (Le Pichon et al 1973). This is consistent with analyses of glacial rebound and lithospheric flexure (McConnell 1968, Walcott 1973, Forsyth 1979), as well as our concept of continental drift.

The important question becomes: How thick is the lithosphere? Or, at least, if we are to construct simple mechanical models for an earthquake cycle, what thickness is appropriate for the elastic layer?

Many investigators agree on a stratified model in which the effective mechanical thickness of the lithosphere depends on time, temperature, strain rate, and deviatoric stress (Melosh 1978b, Forsyth 1979). The upper lithosphere, above approximately the 450° ± 150°C isotherm (Watts 1978), remains essentially elastic and can support loads for 10^8 to 10^9 years; the lower part is elastic-plastic or viscoelastic and relaxes under stresses with durations a few million years. The mechanisms of relaxation in the lower part are similar to those discussed for the asthenosphere (Kirby 1977) but relaxation times are longer for the lithosphere because of lower temperatures. The effective viscosity at the base of the elastic part of the lithosphere is about 10^{26} Poise and in the asthenosphere 10^{21} Poise or less (Melosh 1977, 1978b). At an ocean trench, for example, the long term flexural thickness of the lithosphere may be only 20–40 km (Hanks 1971, Watts & Talwani 1974) because the strain rate associated with the steady component of subduction is low enough and the temperature below 40 km is high enough for the deviatoric stress to stay relaxed. In contrast, at the same trench the nonsteady strain accumulation and release during a rebound cycle lasting tens or hundreds of years occurs in a lithosphere effectively 70 km thick, which is approximately the seismically determined thickness (Kanamori & Press 1970, Le Pichon et al 1973). Similarly, in continental lithosphere the plate thickness for rebound might be the seismic thickness of 110–130 km. Anderson (1971) and Hadley & Kanamori (1977) suggest, however, that in parts of southern California the shallow crust is mechanically decoupled from the lower crust, so that the moving surface plate is much thinner than is commonly inferred from surface waves. Lachenbruch & Sass (1973) suggest a similar decoupling between the shallow crust (15–20 km) around the San Andreas Fault and the more ductile material below in order to explain a low broad heat flow anomaly. However, in this case, the crustal plate is also undergoing permanent shear flow, generating heat. This uncertainty in plate thickness can affect interpretation of surface strain.

Aside from large scale fluidlike flow, which distinguishes the asthenosphere from the lithosphere, a limited viscoelastic relaxation to changes in the stress field can occur within even the shallow lithosphere. In the shallow lithosphere the relaxed configuration is also essentially elastic, distinguished from the unrelaxed state only by a smaller effective rigidity. Hence, a viscoelastic lithosphere exhibiting transient relaxation times on the order of several years would look elastic at seismic frequencies as well as over the longer periods of flexure and isostatic rebound.

A number of relaxation mechanisms can be considered to account for the viscoelastic response. Concentrated plastic flow at grain boundaries is reasonable in much of the lithosphere (below, say, 20–30 km) where

the ratio of absolute temperature T to the melting temperature T_m is greater than one half ($T/T_m > 1/2$). Presumably, motion at grain boundaries could occur while the grains themselves remained essentially elastic, giving to the polycrystalline composite a long term finite strength, yet a short term viscoelastic strain. Pressure solution, a low temperature form of grain boundary diffusion enhanced by water (Tullis 1979), can also relax stresses.

In the shallow crust stress-induced viscous shearing and local squirt of pore fluids (Mavko & Nur 1975, 1979, O'Connell & Budiansky 1977) as well as large scale, regional diffusion (Biot 1941, Nur & Booker 1972) can give a time-dependent deformation qualitatively similar to a viscoelastic response. The regional diffusion might also be enhanced by dilatancy (Nur 1973, Scholz et al 1973).

FAULT CREEP In addition to direct observations of surface fault creep, aseismic fault slip has been invoked at depth in the lithosphere to explain pre- and postseismic surface deformation (Fitch & Scholz 1971, Smith 1974, Thatcher 1975, Brown et al 1977, Thatcher & Rundle 1979). However, very little is known about the detailed stress-strain behavior of the fault zone at any depth. Nason & Weertman (1973) conclude little more than the existence of an upper yield point phenomenon from observations of shallow creep events. In the laboratory transient stable sliding sometimes precedes stick slip on frictional surfaces (Scholz et al 1969, Dieterich 1979a,b) at conditions corresponding to several kilometers depth. At higher temperatures and pressures Stesky (1974) observes a nonlinear stress-strain rate sliding law similar to that expected for solid-state creep. Laboratory measurements on fault gouge and clay have also been made (Engelder et al 1975, Logan & Shimamoto 1976, Summers & Byerlee 1977). The main problem lies in determining what kind of material is representative of a fault zone at depth.

In addition to creep on the primary fault, creep on nearby faults can have an effect on relaxation. Even though the bulk of the crustal material is elastic, slip on secondary faults and fractures makes the crust effectively more compliant. If the slip is creep-like, the change in compliance is gradual, and the overall effect may not be distinguishable from viscoelastic relaxation.

Models

Many features of observed aseismic deformation can be explained by purely elastic models, much like the coseismic models, in which both steady and episodic aseismic slip occur around edges of the rupture surface (Savage & Burford 1970, Thatcher 1975, Shimazaki 1974). In contrast, a

number of authors have attributed the deformation to viscoelastic adjustments, primarily in the asthenosphere (Nur & Mavko 1974, Smith 1974, Rundle & Jackson 1977, Spence & Turcotte 1979, Savage & Prescott 1978a, Thatcher & Rundle 1979). It now appears that the largest postseismic and interseismic strains are dominated by a combination of these two mechanisms although their relative contributions are difficult to resolve and probably vary from region to region. Other mechanisms, for example the diffusion of pore fluids (Nur & Booker 1972), probably affect deformation much less.

STRIKE-SLIP EARTHQUAKES A commonly accepted model for a major earthquake cycle on a strike-slip fault like the San Andreas Fault in California is shown in Figure 6*a*. Two elastic lithospheric plates with thickness H slide past each other with their relative motion occurring across a narrow vertical fault zone. Seismic and geodetic data indicate that seismic slip seldom occurs deeper than ~ 15 km. Therefore, if the concept of strong plates significantly thicker than 15 km is correct, there

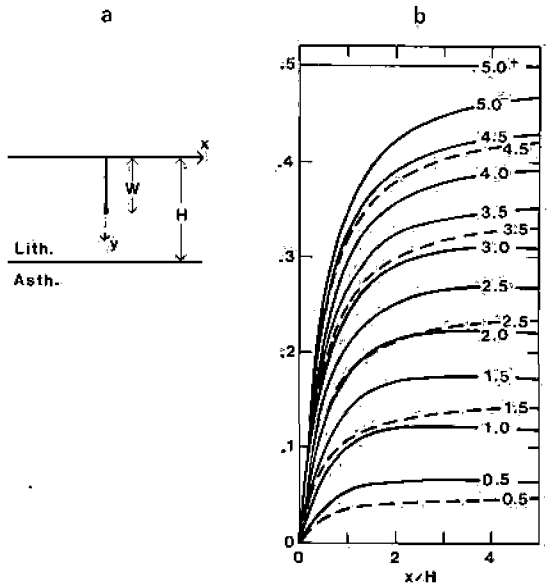

Figure 6 (*a*) Two-dimensional model for a strike-slip earthquake cycle with an elastic lithosphere over a (Maxwell) viscoelastic asthenosphere. (*b*) Surface displacement (solid curves) as a function of distance from the fault, x, for one cycle of periodically occurring earthquake sequences, with $W/H = 0.5$ (after Savage & Prescott 1978a). Displacement is normalized by the seismic slip and is shown relative to the configuration immediately following an earthquake. Curves are labeled with time in increments of $2\eta/\mu$. Dashed curves show the response of an elastic half space to the same earthquake cycle.

can be little doubt that a large amount of aseismic slip at depth is required to accomodate the relative plate offset.

Some of the earliest studies of strain accumulation considered models of deep aseismic slip in an elastic half space (Thatcher 1975, Chinnery 1970, Scholz 1972). Thatcher (1975), for example, explained a rapid episode of postseismic strain ($\sim 1.2\ 10^{-6}$ yr^{-1}) during the 30 years following the 1906 San Francisco earthquake with 3–4 m of slip between depths of 10–30 km. In effect, the rupture, which extended coseismically from the surface to ~ 10 km, gradually deepened by a factor of 2 or 3 during the postseismic period. The resulting postseismic displacement fields would have the form shown in Figure 4*b*, with maximum displacement occurring at a distance of $(10 \cdot 30)^{1/2} = 17.3$ km from the fault, and the far field displacement going to zero. The additional steady component of strain accumulation is simulated with the half space model by uniform slip extending downward to infinity (Savage & Prescott 1978a, Savage et al 1979).

A second series of models attempted to include the effect of a weak fluidlike asthenosphere by considering a plate model with stress-free upper and lower boundaries (Turcotte & Spence 1975, Savage 1975, Spence & Turcotte 1976, Turcotte 1977, Mavko 1977). These models have been criticized (Savage & Prescott 1978a, Spence & Turcotte 1979) for explicitly ignoring the viscous asthenospheric tractions at the base of the plate. It has generally not been recognized, however, that strain rates predicted by plate models with arbitrary nonzero basal tractions under steady motion (if steady motion ever occurs) are exactly the same as for the free plate model (Mavko 1977).

Later studies (Nur & Mavko 1974, Mavko 1977, Rundle & Jackson 1977, Savage & Prescott 1978a, Spence & Turcotte 1979) have included the complete viscoelastic response of the asthenosphere (assuming a Maxwell solid). An example, from Savage & Prescott (1978a), is illustrated in Figure 6*b*, comparing viscoelastic calculations with half-space results. The viscoelastic model assumes steady uniform slip below a depth $W = 0.5\ H$ (where H is the plate thickness) at a rate v equal to the far field plate velocity. In the half-space model the same uniform slip rate extends infinitely deep. Shallower than $W = 0.5\ H$ the fault is usually locked but slips abruptly a uniform amount vT at equally spaced time intervals T. In the example, $T = 5\bar{\tau}_0$ where $\tau_0 = 2\eta/\mu$, η is the asthenospheric viscosity, and μ is the elastic rigidity of the lithosphere and asthenosphere. The unique feature of the viscoelastic model is the rapid postseismic relaxation that causes the displacement rate at a distance $y/H \simeq 2$ to exceed the far field rate early in the cycle. The viscoelasticity tends to concentrate strain accumulation closer to the fault than it is in the half-space model.

Although it is commonly accepted that both slip and asthenospheric effects are important, there is little consensus on their relative contributions. One reason is the uncertainty in plate thickness. Nur & Mavko (1974) and Thatcher (1975) suggested that postseismic viscoelastic effects were not important for earthquakes on the San Andreas Fault, based on an assumed lithospheric thickness of 75–100 km compared to the 15 km coseismic depth. On the other hand, if the thickness of the elastic layer is as small as 20 km (Anderson 1971, Hadley & Kanamori 1977, Lachenbruch & Sass 1973) then the effect may be quite large. A basic problem is our inability to resolve from geodetic observations the difference between deep aseismic slip and distributed viscoelastic relaxation in a layer or half space (Rundle & Jackson 1977, Barker 1976, Savage & Prescott 1978a). In fact, for two-dimensional problems in horizontally layered media, the viscoelastic solution can always be solved using the method of images; that is, a distribution of slip in a uniform half-space model can always be found that precisely duplicates the surface displacement produced by viscoelastic relaxation in one of the buried layers (Savage & Prescott 1978a).

DIP-SLIP EARTHQUAKES Major thrust-type earthquakes at subducting plate margins often rupture through a substantial fraction of the lithosphere, so it is reasonable to expect a large asthenospheric viscoelastic response.

One of the earliest quantitative models for postseismic relaxation in the asthenosphere was the stress guide model introduced by Elsasser (1969, 1971). Patterned after plate tectonics, the model consists of a strong elastic lithospheric plate over a linear viscous fluid asthenosphere. Horizontal displacements, U, in the lithosphere, resulting from long wavelength perturbations in stress, take the form of the diffusion equation,

$$\frac{\delta U}{\delta t} = \frac{h_1 h_2 E}{\eta} \nabla^2 U, \tag{20}$$

Here h_1 and E are the thickness and Young's modulus of the lithosphere and h_2 and η are the thickness and linear viscosity of the asthenosphere, and it is assumed that the scale of lateral variations is large compared to h_1 and h_2. The obvious interpretation (Bott & Dean 1973, Anderson 1975, Savage & Prescott 1978a, Spence & Turcotte 1979) is that localized disturbances (stress drops) associated with earthquakes will diffuse away, qualitatively explaining the transient deformation following some large earthquakes. Anderson (1975) has speculated that this diffusion results in the migration of earthquakes along plate margins. The most important

result is that stress suddenly released at a plate boundary cannot instantaneously affect the whole plate. Disturbances with period T are damped to e^{-1} of their maximum value at a penetration distance δ (skin depth) from the fault:

$$\delta = \left(\frac{Eh_1h_2T}{\pi\eta}\right)^{1/2}. \tag{21}$$

For example, disturbances with period $T = 100$ years (the approximate recurrence time for great earthquakes) are restricted to within a few hundred kilometers of the plate margin, while the interior of a plate is affected only by stresses persisting for a million years or more. This result applies to both strike-slip and dip-slip earthquakes.

The stress guide model has been modified by Melosh (1976) to include a nonlinear fluid asthenosphere, appropriate for long term steady plate motion (Weertman & Weertman 1975, Post & Griggs 1973). The nonlinearity introduces a damped, yet somewhat wavelike, propagation of disturbances which Melosh argues resembles the migration of aftershocks of the 1965 Rat Island, Alaska, earthquake, therefore proving that the asthenosphere is nonlinear. While the asthenosphere is generally considered to be nonlinear, Savage & Prescott (1978b) show that Melosh's (1976) model does not prove it. The short term response of the stress guide model, either linear or nonlinear, is that of an elastic layer over an infinitely rigid half space. Initially, strains are confined to within a layer thickness or so of the fault, and these propagate outward only when the half space begins to relax. A more realistic model, incorporating the initial elastic response of the asthenosphere, results in a larger scale coseismic strain field that subsequently relaxes with less pronounced wavelike propagation. On the other hand, Melosh (1978a) emphasizes that even if the instantaneous elasticity is included, migration effects may still be significant if the asthenosphere is nonlinear. It appears that nonlinear effects on an earthquake cycle have yet to be resolved.

The most successful models of postseismic and interseismic deformation are actually extensions of the purely elastic models developed for coseismic studies. For example, using the solution for a rectangular fault in an elastic half space, Equation (1), Fitch & Scholz (1971) modeled the postseismic deformation following the 1946 Nankaido, Japan, earthquake (Figure 5) with additional forward slip on the down-dip extension of the fault plane and backslip on portions of the coseismic fault plane. A similar model incorporating forward and backslip in an elastic medium was suggested by Scholz & Kato (1978) for deformation following the 1923 Kanto, Japan, earthquake. Brown et al (1977) and Prescott & Lisowski (1977, 1980) used elastic postseismic slip to model deformation following

the 1964 Alaskan earthquake. The requirement of backslip following the Nankaido earthquake was criticized by Nur & Mavko (1974), who suggested instead that the postseismic deformation was dominated by viscoelastic relaxation in the asthenosphere without additional slip. Their model of coseismic slip in an elastic lithosphere (the free surface only crudely approximated) over a linear viscoelastic asthenosphere was the first relaxation model to include both the near field effects of fault dip angle and the initial elastic response of the asthenosphere. Again, the calculation was based on faulting in an elastic medium, with the subsequent viscoelastic response obtained using the correspondence principle (Fung 1965). A similar model, incorporating both slip and asthenospheric relaxation, was developed independently by Smith (1974, 1980).

Recently, a number of numerical models of movements landward of subduction zones, principally in Japan (Bischke 1974, Thatcher & Rundle 1979, Thatcher et al 1980, Smith 1980) and Alaska (Brown et al 1977, Prescott & Lisowski 1977, 1980), have revealed a fairly consistent pattern: rapid episodic slip, both down-dip and up-dip of the coseismic rupture, during the several year postseismic interval and subsidence due to asthenosphere relaxation during the longer interseismic phase. These are illustrated in Figure 5, patterned after the work of Thatcher & Rundle (1979) using an elastic lithosphere over a linear viscoelastic (Maxwell) half space. The curve labeled *CO* shows the vertical coseismic displacement, the elastic half-space response to abrupt slip in the upper portion of the lithosphere. This shallow stress release transfers shear stress to the deeper part of the plate and the asthenosphere. Subsequent aseismic slip down-dip of the rupture and the beginnings of viscoelastic response to both the coseismic and postseismic slip cause the postseismic deformation labeled *POST*. Finally the rapid postseismic deformation merges with the more steady interseismic deformation composed of approximately steady aseismic slip near the bottom of the plate plus viscoelastic subsidence in the asthenosphere, somewhat equivalent to the downward gravitational pull of the slab. Reasonable model parameters for deformation in Japan are a 60 km thick lithosphere and an asthenospheric viscosity of 10^{20}–10^{21} P (Thatcher & Rundle 1979, Thatcher et al 1980).

Disagreements in models are usually in detail only, reflecting our inability to resolve fine details of relaxation. While Thatcher & Rundle (1979) model the asthenosphere under Japan with a viscoelastic half space, Smith (1980) chooses a layered upper mantle with a low viscosity asthenosphere with finite thickness. Thatcher & Rundle prefer postseismic and interseismic slip on a discrete fault plane down-dip of the coseismic rupture; Smith chooses instead distributed viscoelastic relaxation in a low viscosity (10^{19} P) pocket down-dip of the fault plane. The least-understood

effects on deformation are the downward gravitational pull of the slab, buoyancy, and horizontal convergence of the plates during the interseismic period (Thatcher 1979).

HETEROGENEITY IN THE FAULT ZONE

While the emphasis of this review has been on simple quasi-static models, it is important to at least point out the possible role of heterogeneity in stress, material properties, and fault geometry on fault mechanics. Fault models having simple geometries and uniform material properties, like those already discussed, are valuable for understanding large scale low frequency deformation fields associated with an earthquake cycle. However, some heterogeneity is necessary to explain the following fundamental observations: multiple seismic events; high frequency near field ground accelerations; the frequency-magnitude distribution of earthquakes; the termination of rupture (Nur 1978, Andrews 1980, Segall & Pollard 1980).

As discussed by Andrews (1980), rupture termination requires that the difference between the initial shear stress and sliding friction stress vary on the length scale of the rupture, allowing the stress to decrease on much of the slip patch and increase around the borders to stop the rupture (Burridge & Halliday 1971, Andrews 1975). For the same rupture patch, heterogeneity is required on length scales smaller than the rupture length to explain the high frequency ground motion and subsequent smaller earthquakes (Andrews 1978, Nur 1978, Aki 1979). A problem with these frictional models is that the difference between stress and sliding friction becomes smoother with each event until eventually all earthquakes rupture the entire fault. A mechanism is needed to maintain the heterogeneity between stress and friction.

One of the most obvious sources of heterogeneity is fault geometry. The mapped trace of a fault is never a straight cut or break, but often a collection of bent, offset, and sometimes braided strands. Wallace (1973), for example, found that the longest individual fault strands along active portions of the San Andreas fault are about 10 to 18 km long, comparable to the depth of deepest earthquakes. A frequency count of segments by length suggested a distribution of the form $\log N = a + bL$ where N is the number of strands, L is the length, and a and b are constants. Irregular and discontinuous fault traces occur on all scales in nature, for both strike-slip and dip-slip faults, in a variety of rock types and tectonic settings (for a review see Segall & Pollard 1980).

While certain features of the mapped trace geometry may develop as slip propagates upward through unconsolidated sediments, there is some

evidence that faults are discontinuous at appreciable depths (Segall & Pollard 1980). For example, normal faults observed in a South African gold mine are composed of en-echelon segments centimeters to meters in length (McGarr et al 1979). In addition, seismicity patterns often correlate with the surface trace. Aftershocks, at depths of 3–15 km, following the 1966 Parkfield, California, earthquake reflect a 1 km offset in the mapped surface fault trace (Eaton et al 1970b). Bakun et al (1980) and Bakun (1980) report good correlation between the fault trace geometry and epicenter locations (depths 5–8 km), rupture directivity, and aftershock locations on both the San Andreas and Calaveras faults in central California. Hill (1977) and Segall & Pollard (1980) find that earthquake swarms are sometimes localized within fault offsets.

Segall & Pollard (1980) have studied the mechanics of pairs of interacting en-echelon cracks in considerable detail. They suggest that left-stepping offsets on a right lateral fault are sites of increased normal compressive stress that inhibits slip, while right-stepping offsets on right lateral faults have decreased compressive stress, which facilitates slip. Areas of inhibited slip (right lateral, left step) might be sites of strain accumulation and large damaging earthquakes, while areas of enhanced slip (right lateral, right step) might have high seismicity. On a larger scale Mavko (1980) has modeled the interaction of four major faults near Hollister, California, each composed of many individual short segments. Complications in geometry, like large bends, seem to be capable of locking or unlocking sections of the fault which may be important for initiating instability.

SUMMARY

Nearly all fault models are consistent with the concepts of plate tectonics and elastic rebound. Through a combination of remotely applied forces the elastic plates move relative to each other. Whether or not strain accumulates and the way it is released depends on the slip at the common plate boundaries. In terms of the data, the best constrained portion of an earthquake rebound cycle is the rapid coseismic part. Although inelastic deformation in the upper mantle is necessary for long term plate motion and strain accumulation between earthquakes, the short term response of the crust and mantle due to rapid fault slip is essentially elastic. The area, orientation, average slip, and stress drop of the earthquake source can be determined from these coseismic elastic fields using dislocation theory.

A more difficult problem is resolving the sources of aseismic strain. The largest postseismic and interseismic strains appear to be dominated

by a combination of aseismic fault slip and viscoelastic adjustments, primarily in the asthenosphere, while crustal effects, like the diffusion of pore fluids, contribute to a lesser extent.

One of the most promising lines of current research concerns the role of heterogeneity. Although much of our understanding of faulting has resulted from the success of greatly simplified models, heterogeneity in stress, material properties, and geometry is ubiquitous in nature. To some extent, these are a source of noise. For example, variations in crustal stiffness distort strain fields and complicate their interpretation. However, heterogeneity offers perhaps the only explanation for the following fundamental observations: the frequency-magnitude distribution of earthquakes; the termination of rupture; high frequency near field ground accelerations; multiple seismic events.

ACKNOWLEDGMENTS

Frequent discussions with Wayne Thatcher and Jim Savage during the preparation of this paper were extremely helpful. Barbara Mavko, John Langbein, Bill Stuart, and Wayne Thatcher provided useful comments on the manuscript.

Literature Cited

Abramowitz, M., Stegun, I. A. 1964. *Handbook of Mathematical Functions*. Washington, DC: Natl. Bur. Stand. 1046 pp.

Aki, K. 1966. Generation and propagation of G waves from the Niigata earthquake of June 16, 1964, 2, estimation of earthquake moment, released energy, and stress-strain drop from G-waves spectrum. *Bull. Earthquake Res. Inst. Tokyo Univ.* 44:73–88

Aki, K. 1979. Characterization of barriers on an earthquake fault. *J. Geophys. Res.* 84:6140–48

Allen, C. R., Smith, S. W. 1966. Parkfield earthquakes of June 27–29, Monterey and San Luis Obispo Counties, California. Pre-earthquake and post-earthquake surficial displacements. *Bull. Seismol. Soc. Am.* 56:966–67

Anderson, D. L. 1967. The anelasticity of the mantle. *Geophys. J.R. Astron. Soc.* 14:135–64

Anderson, D. L. 1971. The San Andreas fault. *Sci. Am.* 225:52–66

Anderson, D. L. 1975. Accelerated plate tectonics. *Science* 187:1077–79

Ando, M. 1975. Source mechanisms and tectonic significance of historical earthquakes along the Nankai Trough, Japan. *Tectonophysics* 27:119–40

Andrews, D. J. 1975. From antimoment to moment: plain strain models of earthquakes that stop. *Bull. Seismol. Soc. Am.* 65:163–82

Andrews, D. J. 1978. Coupling of energy between tectonic processes and earthquakes. *J. Geophys. Res.* 83:2259–64

Andrews, D. J. 1980. A stochastic fault model—I. static case. *J. Geophys. Res.* 85:3867–77

Ashby, M. F., Verrall, R. A. 1977. Micromechanisms of flow and fracture, and their relevance to the rheology of the upper mantle. *Philos. Trans. R. Soc. London Ser. A* 288:59–95

Bakun, W. H. 1980. Seismic activity (1969 to August 1979) on the southern part of the Calaveras fault in central California. *Bull. Seismol. Soc. Am.* 70:1181–98

Bakun, W. H., Stewart, R. M., Bufe, C. G., Marks, S. M. 1980. Implication of seismicity for failure of a portion of the San Andreas fault. *Bull. Seismol. Soc. Am.* 70:185–202

Barker, T. 1976. Quasi-static motions near the San Andreas fault zone. *Geophys. J.R. Astron. Soc.* 45:689–706

Bilby, B. A., Eshelby, J. D. 1968. Dislocations and the theory of fracture. In *Fracture, An Advanced Treatise*, ed. H.

Liebowitz, pp. 99–182. New York: Academic. 597 pp.
Biot, M. A. 1941. General theory of three dimensional consolidation. *J. Appl. Phys.* 12:155–64
Bischke, R. E. 1974. A model of convergent plate margins based on the recent tectonics of Shikoku, Japan. *J. Geophys. Res.* 79:4845–58
Bott, M. H. P., Dean, D. S. 1973. Stress diffusion from plate boundaries. *Nature* 243:339–41
Brace, W., Byerlee, J. 1970. California earthquakes: why only shallow focus? *Science* 168:1573–75
Bracewell, R. 1965. *The Fourier Transform and its Applications*. New York: McGraw-Hill. 381 pp.
Brown, L. D., Reilinger, R. E., Holdahl, S. R., Balazs, E. I. 1977. Post seismic crustal uplift near Anchorage Alaska. *J. Geophys. Res.* 82:3369–78
Brune, J. N. 1968. Seismic moment, seismicity, and rate of slip along major fault zones. *J. Geophys. Res.* 73:777–84
Burridge, R., Halliday, G. S. 1971. Dynamic shear cracks with friction as models for shallow focus earthquakes. *Geophys. J.* 25:261–83
Burridge, R., Knopoff, L. 1964. Body force equivalents for seismic dislocations. *Bull. Seismol. Soc. Am.* 54:1875–88
Canales, L. 1975. *Inversion of realistic fault models*. PhD thesis. Stanford Univ., Stanford, Calif.
Carter, N. L. 1976. Steady state flow of rocks. *Rev. Geophys. Space Phys.* 14:301–60
Chinnery, M. A. 1961. The deformation of the ground around surface faults. *Bull. Seismol. Soc. Am.* 51:355–72
Chinnery, M. A. 1963. The stress changes that accompany strike slip faulting. *Bull. Seismol. Soc. Am.* 53:921–32
Chinnery, M. A. 1964. The strength of the earth's crust under horizontal shear stress. *J. Geophys. Res.* 69:2085–89
Chinnery, M. A. 1965. The vertical displacements associated with transcurrent faulting. *J. Geophys. Res.* 70:4627–32
Chinnery, M. A. 1967. Theoretical fault models. In *A Symposium on Processes in the Focal Region*, ed. K. Kasahara, A. E. Stevens, pp. 211–23. Ottawa: Dominion Astrophys. Obs.
Chinnery, M. A. 1970. Earthquake displacement fields. In *Earthquake Displacement Fields and the Rotation of the Earth*, ed. L. Mansinha et al, pp. 17–38. Dordrecht: Reidel. 308 pp.
Chinnery, M. A., Jovanovich, D. B. 1972. Effect of earth layering on earthquake displacement fields. *Bull. Seismol. Soc. Am.* 62:1629–39
Chinnery, M. A., Petrak, J. A. 1967. The dislocation fault model with a variable discontinuity. *Tectonophysics* 5:513–29
Christensen, R. M. 1971. *Theory of Viscoelasticity*. New York: Academic. 245 pp.
Claerbout, J. F. 1976. *Fundamentals of Geophysical Data Processing*. New York: McGraw-Hill. 274 pp.
Dieterich, J. H. 1974. Earthquake mechanisms and modeling. *Ann. Rev. Earth Planet. Sci.* 2:275–301
Dieterich, J. H. 1979a. Modeling of rock friction, 1, experimental results and constitutive equations. *J. Geophys. Res.* 84:2161–68
Dieterich, J. H. 1979b. Modeling of rock friction, 2, simulation of preseismic slip. *J. Geophys. Res.* 84:2169–76
Dunbar, W. S. 1977. *The determination of fault models from geodetic data*. PhD thesis. Stanford Univ., Stanford, Calif.
Eaton, J. P., Lee, W. H. K., Pakiser, L. C. 1970a. Use of microearthquakes in the study of the mechanics of earthquake generation along the San Andreas fault in central California. *Tectonophysics* 9:259–82
Eaton, J. P., O'Neill, M. E., Murdock, J. N. 1970b. Aftershocks of the 1966 Parkfield-Cholame, California, earthquake: a detailed study. *Bull. Seismol. Soc. Am.* 60:1151–97
Elsasser, W. M. 1969. Convection and stress propagation in the upper mantle. In *The Application of Modern Physics to the Earth and Planetary Interiors*, ed. S. K. Runcorn, pp. 223–45. New York: Wiley
Elsasser, W. M. 1971. Two-layer model of upper-mantle circulation. *J. Geophys. Res.* 76:4744–53
Engelder, J. T., Logan, J. M., Handin, J. 1975. The sliding characteristics of sandstone on quartz fault-gouge. *Pure Appl. Geophys.* 113:69–86
Erdelyi, A., Magnus, W., Oberhettinger, F., Tricomi, F. G. 1954. *Tables of Integral Transforms, vol. 2*. New York: McGraw-Hill. 451 pp.
Eshelby, J. D. 1957. The determination of the elastic field of an ellipsoidal inclusion and related problems. *Proc. R. Soc. London Ser. A* 241:376–96
Fitch, T., Scholz, C. H. 1971. Mechanism of underthrusting in southwest Japan: a model of convergent plate interactions. *J. Geophys. Res.* 80:1444–47
Forsyth, D. W. 1979. Lithospheric flexure. *Rev. Geophys. Space Phys.* 17:1109–14

Freund, L. B. 1979. The mechanics of dynamic shear crack propagation. *J. Geophys. Res.* 84:2199–2209
Fung, Y. C. 1965. *Foundations of Solid Mechanics*. Englewood Cliffs, NJ: Prentice-Hall. 525 pp.
Gordon, R. B. 1965. Diffusion creep in the earth's mantle. *J. Geophys. Res.* 70:2413–18
Goulty, N. R., Gilman, R. 1978. Repeated creep events on the San Andreas fault near Parkfield, California, recorded by a strainmeter array. *J. Geophys. Res.* 83:5415–19
Hadley, D., Kanamori, H. 1977. Seismic structures of the Transverse Ranges, California. *GSA Bull.* 88:1469–78
Hanks, T. C. 1971. The Kuril trench-Hokkaido rise system: Large shallow earthquakes and simple models of deformation. *Geophys. J. R. Astron. Soc.* 23:173–89
Heard, H. C. 1976. Comparison of the flow properties of rocks at crustal condition. *Philos. Trans. R. Soc. London Ser. A* 283:173–89
Hill, D. P. 1977. A model for earthquake swarms. *J. Geophys. Res.* 82:1347–52
Jackson, D. D., Anderson, D. L. 1970. Physical mechanisms of seismic wave attenuation. *Rev. Geophys. Space Phys.* 8:1–63
Kanamori, H. 1973. Mode of strain release associated with major earthquakes in Japan. *Ann. Rev. Earth Planet. Sci.* 1:213–39
Kanamori, H., Anderson, D. L. 1975. Amplitude of the earth's free oscillations and long period characteristics of the earthquake source. *J. Geophys. Res.* 80:1075–78
Kanamori, H., Cipar, J. 1974. Focal processes of the great Chilean earthquake. *Phys. Earth Planet. Inter.* 9:128–36
Kanamori, H., Press, F. 1970. How thick is the lithosphere? *Nature* 226:330–31
Kasahara, K. 1957. The nature of seismic origins as inferred from seismological and geodetic observations (1). *Bull. Earthquake Res. Inst. Tokyo Univ.* 35:473–532
Kasahara, K. 1958. Physical conditions of earthquake faults as deduced from geodetic data. *Bull. Earthquake Res. Inst. Tokyo Univ.* 36:455–64
Ke, T. S. 1947. Experimental evidence of the viscous behavior of grain boundaries in metals. *Phys. Rev.* 71:533
King, C.-Y., Nason, R. D., Tocher, D. 1973. Kinematics of fault creep. *Philos. Trans. R. Soc. London Ser. A* 274:355–60
King, N. E., Savage, J. C., Lisowski, M., Prescott, W. H. 1980. Preseismic and coseismic deformation associated with the Coyote Lake, California, earthquake. *J. Geophys. Res.* In press
Kirby, S. H. 1977. State of stress in the lithosphere: inferences from the flow laws of olivine. *Pure Appl. Geophys.* 115:245–58
Knopoff, L. 1958. The energy release in earthquakes. *Geophys. J.* 1:44–52
Lachenbruch, A. H., Sass, J. H. 1973. Thermo-mechanical aspects of the San Andreas Fault system. In *Proc. Conf. Tectonic Problems of the San Andreas Fault System*, ed. R. L. Kovach, A. Nur, pp. 192–205. Stanford, Calif: Stanford Univ. Publications
Langbein, J. O. 1980. An interpretation of episodic slip on the Calaveras fault near Hollister, California. *J. Geophys. Res.* In press
Lensen, G. 1970. Elastic and non-elastic surface deformation in New Zealand. *Bull. N.Z. Soc. Earthquake Eng.* 3:131–43
Le Pichon, X., Francheteau, J., Bonnin, J. 1973. *Plate Tectonics*. New York: Elsevier. 300 pp.
Logan, J. M. 1979. Brittle phenomena. *Rev. Geophys. Space Phys.* 17:1121–31
Logan, J. M., Shimamoto, T. 1976. The influence of calcite gouge on the frictional sliding of Tennessee sandstone (abstract). *EOS, Trans. Am. Geophys. Union* 57:1011
Love, A. E. H. 1944. *A Treatise on the Mathematical Theory of Elasticity*. New York: Dover. 643 pp.
Madariaga, R. 1979. On the relation between seismic moment and stress drop in the presence of stress and strength heterogeneity. *J. Geophys. Res.* 84:2243–50
Mahrer, K. 1978. *Strike slip faulting, models for deformation in a nonuniform crust*. PhD thesis. Stanford Univ., Stanford, Calif. 190 pp.
Mahrer, K. D., Nur, A. 1979. Strike slip faulting in a downward varying crust. *J. Geophys. Res.* 84:2296–2302
Maruyama, T. 1964. Statical elastic dislocations in an infinite and semi-infinite medium. *Bull. Earthquake Res. Inst. Tokyo Univ.* 42:289–368
Matuzawa, T. 1964. *Study of Earthquakes*. Tokyo: Uno Shoten
Mavko, G. 1977. *Time dependent fault mechanics and wave propagation in rocks*. PhD thesis. Stanford Univ., Stanford, Calif.
Mavko, G. 1978. Large scale quasi-static fault models. In *Proc. Conf. III Fault Mechanics and Its Relation to Earthquake Prediction*, ed. J. F. Evernden, pp. 339–412. Menlo Park, Calif: US Geol. Surv.
Mavko, G. M. 1980. The influence of

local moderate earthquakes on creep rate near Hollister, California, *Earthquake Notes* 50:71

Mavko, G., Nur, A. 1975. Melt squirt in the asthenosphere. *J. Geophys. Res.* 80:1444–47

Mavko, G., Nur, A. 1978. The effect of non-elliptical cracks on the compressibility of rocks. *J. Geophys. Res.* 83: 4459–68

Mavko, G. M., Nur, A. 1979. Wave attenuation in partially saturated rocks. *Geophysics* 44:161–78

McConnell, R. K. 1968. Viscosity of the mantle from relaxation time spectra of isostatic adjustment. *J. Geophys. Res.* 73:7089–7105

McGarr, A., Pollard, D., Gay, N. C., Ortlepp, W. D. 1979. Observations and analysis of structures in exhumed mines. In *Proc. Conf. VIII Analysis of Actual Fault Zones in Bedrock*, ed. J. F. Evernden, pp. 101–20. Menlo Park, Calif.: US Geol. Surv. 594 pp.

Melosh, H. J. 1976. Nonlinear stress propagation in the earth's upper mantle. *J. Geophys. Res.* 81:5621–32

Melosh, H. J. 1977. Shear stress on the base of a lithospheric plate. *Pure Appl. Geophys.* 115:429–39

Melosh, H. J. 1978a. Reply. *J. Geophys. Res.* 83:5009–10

Melosh, H. J. 1978b. Dynamic support of the outer rise. *Geophys. Res. Lett.* 5:321–24

Mescherikov, J. A. 1968. Recent crustal movements in seismic regions: geodetic and geomorphic data. *Tectonophysics* 6:29–39

Mindlin, R. D., Cheng, D. H. 1950. Nuclei of strain in the semi-infinite solid. *J. Applied Phys.* 21:926–30

Muskhelishvili, N. I. 1953. *Some Basic Problems of the Mathematical Theory of Elasticity*. Groningen, Holland: Noordhoff. 704 pp.

Nakamura, K., Tsuneishi, Y. 1967. Ground cracks at Matsushiro probably of strike-slip fault origin. *Bull. Earthquake Res. Inst. Univ. Tokyo.* 45:417–72

Nason, R. D. 1973. Fault creep and earthquakes on the San Andreas Fault. In *Proc. Conf. Tectonic Problems of the San Andreas Fault System*, ed. R. L. Kovach, A. Nur, pp. 275–3895. Stanford, Calif.: Stanford Univ. Publications

Nason, R., Weertman, J. 1973. A dislocation theory analysis of fault creep events. *J. Geophys. Res.* 78:7745–51

Nur, A. 1973. Role of pore fluids in faulting. *Philos. Trans. R. Soc. London Ser. A.* 274:297–304

Nur, A. 1978. Nonuniform friction as a basis for earthquake mechanics. *Pure Appl. Geophys.* 116:964–91

Nur, A., Booker, J. R. 1972. Aftershocks caused by pore fluid flow? *Science* 175:885–87

Nur, A., Mavko, G. 1974. Postseismic viscoelastic rebound. *Science* 183:204–6

O'Connell, R. J., Budiansky, B. 1977. Viscoelastic properties of fluid-saturated cracked solids. *J. Geophys. Res.* 82:5719–35

Petrak, J. A. 1965. *Some theoretical implications of strike-slip faulting*. M.A. thesis. Univ. British Columbia, Vancouver, B.C.

Pfluke, J. H. 1978. Slow earthquakes and very slow earthquakes. In *Proc. Conf. III Fault Mechanics and Its Relation to Earthquake Prediction*, ed. J. F. Evernden, pp. 447–468. Menlo Park, Calif: US Geol. Surv.

Post, R., Griggs, D. 1973. The earth's mantle: evidence of non-Newtonian flow. *Science* 181:1242–44

Prescott, W. H., Lisowski, M. 1977. Deformation at Middleton Island, Alaska, during the decade after the Alaska earthquake of 1964. *Bull. Seismol. Soc. Am.* 66:1013–16

Prescott, W. J., Lisowski, M. 1980. Vertical deformation at Middleton Island *Earthquake Notes* 50:72 (Abstr.)

Press, F. 1965. Displacements, strains, and tilts at teleseismic distances. *J. Geophys. Res.* 70:2395–2412

Reid, H. F. 1910. The mechanics of the earthquake. In *The California Earthquake of April 18, 1906. Rep. State Earthquake Invest. Comm.* Washington, DC: Carnegie Inst.

Rudnicki, J. W. 1980. Fracture mechanics applied to the earth's crust. *Ann. Rev. Earth Planet. Sci.* 8:489–525

Rundle, J. B., Jackson, D. D. 1977. A viscoelastic relaxation model for post-seismic deformation from the San Francisco earthquake of 1960. *Pure Appl. Geophys.* 115:401–11

Rybicki, K. 1971. The elastic residual field of a very long strike-slip fault in the presence of a discontinuity. *Bull. Seismol. Soc. Am.* 61:79–92

Rybicki, K., Kasahara, K. 1977. A strike-slip fault in a laterally inhomogeneous medium. *Tectonophysics* 42:127–38

Sacks, I. S., Suyehiro, S., Linde, A. T., Snoke, J. A. 1977. The existence of slow earthquakes and the redistribution of stress in seismically active regions. *EOS, Trans. Am. Geophys. Union.* 58:437

Savage, J. C. 1975. Comment on "An analysis of strain accumulation on a strike

slip fault" by D. L. Turcotte and D. A. Spence. *J. Geophys. Res.* 80:4111–14
Savage, J. C. 1978. Comment on "Strain accumulation and release mechanism of the 1906 San Francisco earthquake" by W. Thatcher. *J. Geophys. Res.* 83:5487–89
Savage, J. C., Burford, R. O. 1970. Accumulation of tectonic strain in California. *Bull. Seismol. Soc. Am.* 60:1877–96
Savage, J. C., Hastie, L. M. 1966. Surface deformation associated with dip-slip faulting. *J. Geophys. Res.* 71:4897–4904
Savage, J. C., Prescott, W. H. 1978a. Asthenospheric readjustment and the earthquake cycle. *J. Geophys. Res.* 83:3369–76
Savage, J. C., Prescott, W. H. 1978b. Comment on "Nonlinear stress propagation in the earth's upper mantle" by H. J. Melosh. *J. Geophys. Res.* 83:5005–8
Savage, J. C., Prescott, W. H., Lisowski, M., King, N. 1979. Geodolite measurements of deformation near Hollister, California, 1971–1978. *J. Geophys. Res.* 84:7599–7615
Scholz, C. H. 1972. Crustal movements in tectonic areas. *Tectonophysics* 14:201–17
Scholz, C. H., Kato, T. 1978. The behavior of a convergent plate boundary: crustal deformation in the South Kanto district, Japan. *J. Geophys. Res.* 83:783–97
Scholz, C. H., Sykes, L. R., Aggarwal, Y. P. 1973. Earthquake prediction: a physical basis. *Science* 181:803–10
Scholz, C. H., Wyss, M., Smith, S. W. 1969. Seismic and aseismic slip on the San Andreas fault. *J. Geophys. Res.* 74:2049–69
Segall, P., Pollard, D. D. 1980. Mechanics of discontinuous faults. *J. Geophys. Res.* 85:4337–50
Shimazaki, K. 1974. Preseismic crustal deformation caused by an underthrusting oceanic plate, in eastern Hokkaido, Japan. *Phys. Earth Planet. Inter.* 8:148–57
Smith, A. T. 1974. Time-dependent strain accumulation and release at island arcs. *EOS, Trans. Am. Geophys. Union* 55:427
Smith, A. T. 1980. *Final Technical Report: Earthquake risk analysis using numerical and stochastic models of time-dependent strain fields.* Santa Cruz, Calif: Univ. Calif.
Smith, S. W., Wyss, M. 1968. Displacement on the San Andreas fault initiated by the 1966 Parkfield earthquake. *Bull. Seismol. Soc. Am.* 58:1955–74
Sneddon, I. N., Lowengrub, M. 1969. *Crack Problems in the Classical Theory of Elasticity.* New York: Wiley. 221 pp.
Spence, D. A., Turcotte, D. L. 1976. An elastostatic model of stress accumulation on the San Andreas fault. *Proc. R. Soc. London Ser. A* 349:319–41
Spence, D. A., Turcotte, D. L. 1979. Viscoelastic relaxation of cyclic displacements on the San Andreas fault. *Proc. R. Soc. London Ser. A* 365:121–44
Starr, A. T. 1928. Slip in a crystal and rupture in a solid due to shear. *Proc. Camb. Philos. Soc.* 24:489–500
Steketee, J. A. 1958a. On Volterra's dislocations in a semi-infinite medium. *Can. J. Phys.* 36:192–204
Steketee, J. A. 1958b. Some geophysical applications of the elasticity theory of dislocations. *Can. J. Phys.* 36:1168–97
Stesky, R. M. 1974. Steady-state creep law for frictional sliding at high temperature and pressure. *EOS, Trans. Am. Geophys. Union* 55:428
Stuart, W. D. 1978. Review of theories for earthquake instabilities. In *Proc. Conf. III Fault Mechanics and Its Relation to Earthquake Prediction*, ed. J. F. Evernden, pp. 541–88. Menlo Park, Calif: US Geol. Surv.
Stuart, W. D. 1979. Quasi-static earthquake mechanics. *Rev. Geophys. Space Phys.* 17:1115–20
Stuart, W. D., Mavko, G. M. 1979. Earthquake instability on a strike-slip fault. *J. Geophys. Res.* 84:2153–60
Summers, R., Byerlee, J. D. 1977. A note on the effect of fault gouge composition on the stability of frictional sliding. *Int. J. Rock Mech. Min. Sci.* 14:155–60
Thatcher, W. 1975. Strain accumulation and release mechanism of the 1906 San Francisco earthquake. *J. Geophys. Res.* 80:4862–72
Thatcher, W. 1978. Reply. *J. Geophys. Res.* 83:5490–92
Thatcher, W. 1979. Crustal movements and earthquake-related deformation. *Rev. Geophys. Space Phys.* 17:1403–10
Thatcher, W., Matsuda, T., Kato, T., Rundle, J. B. 1980. Lithospheric loading by the 1896 Riku-U earthquake, northern Japan: implications for plate flexure and asthenospheric rheology. *J. Geophys. Res.* In press
Thatcher, W., Rundle, J. B. 1979. A model for the earthquake cycle in the underthrust zones. *J. Geophys. Res.* 84:5540–56
Tullis, J. A. 1979. High temperature deformation of rocks and minerals. *Rev. Geophys. Space Phys.* 17:1137–54
Turcotte, D. L. 1977. Stress accumulation and release on the San Andreas fault. *Pure Appl. Geophys.* 115:413–25
Turcotte, D. L., Spence, D. A. 1975. Reply to comments by J. C. Savage, *J. Geophys. Res.* 80:4115

US Geological Survey. 1980. *Professional Paper, The Imperial Valley Earthquake of October 15, 1979*. Menlo Park, Calif: US Geol. Surv.

Walcott, R. I. 1973. Structure of the earth from glacio-isostatic rebound. *Ann. Rev. Earth Planet. Sci.* 1:15–37

Wallace, R. E. 1973. Surface fracture patterns along the San Andreas fault. In *Proc. Conf. Tectonic Problems of the San Andreas Fault System*, ed. R. L. Kovach, A. Nur. Stanford Univ. Publications

Walsh, J. B. 1969. A new analysis of attenuation in partially melted rock. *J. Geophys. Res.* 74:4333

Watts, A. B. 1978. An analysis of isostasy in the world's oceans, 1, Hawaiian-Emperor seamount chain. *J. Geophys. Res.* 83: 5989–6004

Watts, A. B., Talwani, M. 1974. Gravity anomalies seaward of deep sea trenches and their tectonic implications. *Geophys. J.R. Astron. Soc.* 36:57–90

Weertman, J. 1964. Continuum distribution of dislocations on faults with finite friction. *Bull. Seismol. Soc. Am.* 54:1035–58

Weertman, J. 1965. Relationship between displacements on a free surface and the stress on a fault. *Bull. Seismol. Soc. Am.* 55:945–53

Weertman, J. 1978. Creep laws for the mantle of the earth. *Philos. Trans. R. Soc. London Ser. A* 288:9–26

Weertman, J., Weertman, J. R. 1964. *Elementary Dislocation Theory*. London: Macmillan. 213 pp.

Weertman, J., Weertman, J. R. 1975. High temperature creep of rock and mantle viscosity. *Ann. Rev. Earth Planet. Sci.* 3:293–315

Wyss, M., Brune, J. N. 1968. Seismic moment, stress, and source dimensions in the California-Nevada region. *J. Geophys. Res.* 73:4681–94

Zener, C. 1948. *Elasticity and Anelasticity of Metals*. Chicago: Univ. of Chicago Press. 170 pp.